Charge-Induced Anisotropic Distortions of Semiconducting and Metallic Carbon Nanotubes

Yu. N. Gartstein,[1] A. A. Zakhidov,[2] and R. H. Baughman[2]
[1]*Xerox Corporation, 147-59B, 800 Phillips Road, Webster, New York 14580*
[2]*UTD NanoTech Institute, University of Texas at Dallas, Richardson, Texas 75083*
(Received 5 February 2002; published 9 July 2002)

To accommodate extra electrons or holes injected into a single-wall carbon nanotube, carbon-carbon bonds adjust their lengths. Resulting changes in carbon-nanotube length as a function of charge injection provide the basis for electromechanical actuators. We show that a key mechanism at low injection levels, modulation of electron kinetic energy, provides nanotube deformations that are both anisotropic and strongly dependent on nanotube structure. Nanotubes can exhibit both expansion and contraction, as well as nonmonotonic size changes. The magnitude of the actuation response of semiconducting carbon nanotubes may be substantially larger than that of graphite.

DOI: 10.1103/PhysRevLett.89.045503 PACS numbers: 61.46.+w, 71.38.–k, 73.22.–f, 85.85.+j

Carbon nanotubes are particularly interesting nanoscopic systems [1] whose electronic and mechanical properties have been the subject of numerous studies and are attractive for diverse applications [2,3]. One of the proposals is to use carbon single-wall nanotubes (SWNTs) as electrochemically driven electromechanical actuators. In these demonstrated devices, large electrochemical charge injection can result from the high surface area of nanotube assemblies [4]. The charge injection produces the electromechanical actuation. Actuator strains of above 1% have been observed [3], which is about 10 times that of ferroelectrics. This high strain indicates the potential for obtaining order of magnitude advantages over any prior-art actuator technologies for directly converting electrical energy to mechanical energy. Currently available nanotube sheets and long fibers comprise bundles of SWNTs, each bundle containing from 30 to 100 of SWNTs of various internal geometries, or chiral vectors (N, M) [1]: from zigzag $(N, 0)$ to armchair (N, N) tubes. The observed actuation is likely to be an average from different SWNTs. Improved synthetic methods are expected to eventually make it possible to use SWNTs of selected types in actuators [5]. The purpose of this Letter is to predict the actuator strains that would result for different types of SWNTs by studying a simplified electron-lattice model. Since Coulombic effects are ignored in this model, our results are restricted to low charge injection levels. We demonstrate that SWNTs exhibit quite a unique picture of electromechanical actuation that strongly depends on (N, M). The magnitude of the actuator response of individual carbon nanotubes can be appreciably larger than that of graphite, presenting an exciting opportunity of enhanced actuation.

Suppose one adds δn extra electrons per carbon atom to a SWNT. How would interatomic distances be affected? Here we study the contribution to bond length changes arising from the modulation of electron hopping integrals t by lattice distortions. The basic illustration is very simple: if an extra electron or hole is added to a half-filled two-site system, this would cause an expansion of the intersite bond by $\delta d = \alpha/K$, where K is the elastic constant and the hopping integral is modulated as $\delta t = -\alpha \delta d$ [6]. We show that manifestations of this relaxation mechanism can produce surprisingly different overall dimensional changes for carbon nanotubes having different values of N and M.

An important issue is the relationship of effects due to electron ($\delta n > 0$) versus hole ($\delta n < 0$) doping. Addition of electrons or holes to a *half-filled* system with *charge conjugation symmetry* (CCS) would result in the same dimensional changes: the response is an even function of δn. The two-site system possesses CCS. Tight binding models of graphite and carbon nanotubes in the nearest neighbor hopping (NNH) approximation are also CC symmetric. On the other hand, experiments show [4] that the dimensional effect can change its sign with δn at small δn. To allow for such a CCS breaking, we explicitly consider second order hopping (SOH) (e.g., [7]), with electronic energy bands acquiring the form

$$\epsilon_{\pm}(\vec{k}) = \tau(\vec{k}) \pm \xi(\vec{k}) \qquad (1)$$

for the conduction and valence bands, respectively. $\xi(\vec{k})$ originates from the NNH between carbon atoms and $\tau(\vec{k})$ from the SOH. We assume that electrons/holes added to the system are accommodated in the band states of the lowest available excitation energies [8]. The dimensional effects then appear as a result of variation of the band parameters by the lattice displacements.

The lattice distortions in this Letter are restricted to uniform length modulations of the three types of bonds (denoted d_a, d_b, and d_c) , as shown in Fig. 1. Correspondingly, there are three types of NNH integrals: t_a, t_b, t_c, and three types of SOH integrals: t_1, t_2, and t_3. The coupling constant α describes the modulation of NNH, e.g., $t_a = 1 - \alpha \delta d_a$ [11]; the corresponding constant for SOH is denoted β ($\beta/\alpha \sim 0.1$). Anisotropic distortions play an important role in nanotubes. This was first recognized by Kane and Mele [12] who showed how anisotropic fluctuations introduce a symmetry breaking and serve as strong

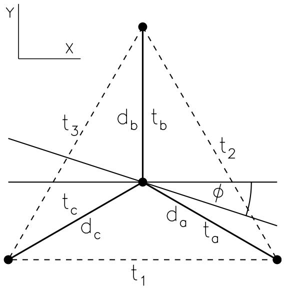

FIG. 1. Four carbon atoms of the repeating motif are depicted with the three types of bonds d_a, d_b, and d_c and the corresponding NNH and SOH integrals. Also shown is the nanotube axis at the angle ϕ with the x axis.

scatterers of quantum particles. We explicitly define the *isotropic* mode S and two *anisotropic* modes A_1 and A_2 so that individual bond length changes are expressed as

$$\begin{cases} -\alpha\delta d_a = S/3 - A_1/2\sqrt{3} - A_2/2, \\ -\alpha\delta d_b = S/3 + A_1/\sqrt{3}, \\ -\alpha\delta d_c = S/3 - A_1/2\sqrt{3} + A_2/2. \end{cases} \tag{2}$$

To gain physical insight into the problem, let us turn attention to not too small nanotubes. Then the low excitation energy region is close to special points in the momentum space, where the gap of the (isotropic) graphene spectrum vanishes [1,12], and one can use expansions of the exact band energies. For certainty, we choose the special point $\vec{K} = (4\pi/3, 0)$ and measure all momenta $\vec{k} = (k_x, k_y)$ from that point. The resulting expansions (τ_0 is the equilibrium value of τ) are

$$\tau(\vec{k}) = \tau_0(\vec{k}) + \sqrt{3}(\beta/\alpha)[S + 3(k_x A_1 + k_y A_2)/4], \tag{3}$$

$$\begin{aligned} \xi^2(\vec{k}) = {} & (3 + 2S - 2\sqrt{3}A_1)(k_x - A_1)^2/4 \\ & + (3 + 2S + 2\sqrt{3}A_1)(k_y - A_2)^2/4 \\ & + \sqrt{3}A_2(k_x - A_1)(k_y - A_2). \end{aligned} \tag{4}$$

For the (N, M) tube, the chiral angle ϕ (Fig. 1) is defined through $\sin\phi = (N - M)/2C_h$, where the tube circumference $C_h = (N^2 + M^2 + NM)^{1/2}$. We consider ϕ belonging to the interval between 0 (armchair tubes) and $\pi/6$ (zigzag tubes). Of extreme importance is the divisibility of $N - M$ by 3; the "remainder" $q = 0, \pm 1$ is introduced by

$$N - M = 3m + q, \tag{5}$$

where m is the appropriate integer. The electron momenta can lie only on a set of quantization lines; the one most closely approaching the special point is described by $k_x \sin\phi + k_y \cos\phi = -2\pi q/3C_h = K_0$. The lowest ξ energy in the equilibrium system is $\xi_0 = (3K_0^2/4)^{1/2} = \pi|q|/\sqrt{3}C_h$, finite for semiconducting nanotubes ($|q| = 1$) and zero for metallic ones ($q = 0$).

The new configuration of the doped system is obtained by minimizing the variable part of the total adiabatic energy *per carbon atom:* $\delta U = E_{\mathrm{el}} + U_{\mathrm{lat}}$. For simplicity, here we consider only one nearest neighbor elastic constant K so that the lattice energy reads $U_{\mathrm{lat}} = K[S^2/3 + (A_\parallel^2 + A_\perp^2)/2]/4\alpha^2$, where distortions A_1 and A_2 are replaced with their projections on axes parallel ($A_\parallel$) and perpendicular ($A_\perp$) to the quantization lines:

$$A_\parallel = A_1 \cos\phi - A_2 \sin\phi,$$

$$A_\perp = A_1 \sin\phi + A_2 \cos\phi.$$

The electronic part of the energy is taken as

$$E_{\mathrm{el}} = \sqrt{3}(\beta/\alpha)S\delta n + (1/f)\int_0^{\delta k} \xi(k)\, dk, \tag{6}$$

where only one practically non-negligible term from (3) is left. The coefficient f relates the boundary δk of the occupied states in the momentum space to the charge injection level: $\delta k = f|\delta n|$, $f = \pi C_h/\sqrt{3}$ (with account of band degeneracy).

The interesting physics occurs in the NNH part. One-dimensional (momentum k) "ξ bands" along the quantization lines are obtained from (4) and have the familiar Dirac form

$$\xi^2(k) = \Delta^2 + v_\parallel^2 k^2, \tag{7}$$

where the gap parameter

$$\Delta = v_\perp |K_0 - A_\perp| \tag{8}$$

and the effective Fermi velocities

$$v_\parallel = v_F - A/2, \qquad v_\perp = v_F + A/2. \tag{9}$$

Here $v_F = \sqrt{3}/2 + S/2\sqrt{3}$ and $A = A_\parallel \cos 3\phi + A_\perp \sin 3\phi$. Equations (8) and (9) illustrate a significant difference between the effects of the isotropic and anisotropic distortions. The major effect from the anisotropic modes is the displacement of the special point [12,13], or modulation of the gap by $A_\perp$. There is also an effect from modulation of $v_\perp$ in (8) by all modes, but it is proportional to a small quantity K_0. Anisotropic modes actually split the Fermi velocity into $v_\perp$ and $v_\parallel$ (9) which leads to an additional interplay of the effects upon increase of the injection level.

The experimentally observed macroscopic changes can be found from the definition (2) and Fig. 1. So for the relative changes of the tube length $\delta L/L = \gamma_\parallel$ and radius $\delta R/R = \gamma_\perp$, one obtains

$$-(\alpha d)\gamma_{\parallel,\perp} = S/3 \mp A/2\sqrt{3}. \tag{10}$$

As an instructive example, we first analyze the effects linear in δn. Then the integral in (6) reduces to $\Delta|\delta n|$ and one easily finds optimal distortions that, when put into (10), lead to simple expressions:

$$\begin{cases} \gamma_\parallel = (\alpha/Kd)[2\sqrt{3}\beta/\alpha \mp q \sin 3\phi]\delta n, \\ \gamma_\perp = (\alpha/Kd)[2\sqrt{3}\beta/\alpha \pm 4\pi|q|/3\sqrt{3}C_h \\ \qquad \pm q \sin 3\phi]\delta n, \end{cases} \tag{11}$$

where upper/lower signs correspond to electron/hole doping. A notable feature of Eqs. (11) are the terms proportional to the factor $q = 0, \pm 1$ (5) which leads to responses oscillating as a function of $N - M$. This is reflected in Fig. 2 (that figure also displays some other effects described below; representative numerical parameters used are $\alpha/Kd = 0.2$ and $\beta/\alpha = 0.1$). The large scale anisotropy of the response is clear from comparing the panels. The found oscillatory dependence of actuator strain is consistent with the picture of the band gap modulation described recently for deformed nanotubes [14]. The second order effect ($\propto \beta$) leads to a plain shift of the "zero line" and to CCS breaking between electron and hole doping. For metallic systems with $q = 0$, this term may be dominating. The leading response from the NNH in that case is $\propto \delta n^2$ as arising from the modulation of $v_\parallel$ in (9). This brings an additional term $(\alpha/Kd) f \delta n^2/\sqrt{3}$ into $\gamma_\parallel$ in (11). So for the (10, 10) tube at $\delta n = 0.01$, the latter quadratic term is about half of the contribution from the SOH.

The systems above had purely spontaneous anisotropy induced by the interaction of extra charges with the lattice. In reality, the undoped system itself can already be anisotropic. An important source of such "external" anisotropy is the curvature of nanotubes. An elegant analysis of the curvature effects was, e.g., given by Kane and Mele [12]. Curvature induced anisotropy is described the same way as anisotropic modes: one needs to replace $A_\perp \rightarrow A_\perp + A_e \sin 3\phi$, $A_\parallel \rightarrow A_\parallel + A_e \cos 3\phi$ in Eqs. (8) and (9) (but not in the elastic energy). From Ref. [12] we deduce the value $A_e = -\pi^2/4\sqrt{3}\, C_h^2$. Appearance of a small gap $\propto A_e$ drastically changes the response of quasimetallic nanotubes for very low doping levels. However, the role of a small gap quickly diminishes upon an increase of the doping level. So Fig. 2 displays effects (10) with optimal distortions found by numerical minimization of δU for the electron doping level $\delta n = 0.5\%$. The figure shows not only the linear effects (11) but also the interplay of effects coming from the curvature and from the filling of the electron states above the band edge.

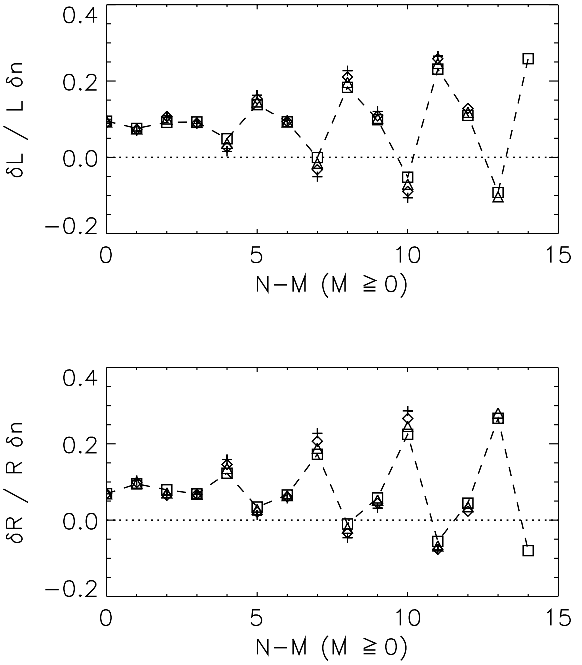

FIG. 2. Reduced dimensional distortions (10) for the electron doping level $\delta n = 0.005$. Shown are results for four "families" of carbon nanotubes: with $N = 11$ (crosses), 12 (diamonds), 13 (triangles), and 14 (squares). Connected with broken lines are the square data points. The upper panel shows changes in the nanotube length, and the lower changes in nanotube radius.

A further increase of the injection level leads to charges starting to fill in the higher lying energy bands. The lowest critical densities are found as $\delta n_{\rm met} = 2\sqrt{3}/C_h^2$, $\delta n_{\rm sem} = 2/C_h^2$. This yields, e.g., $\delta n_{\rm met} \simeq 1.2\%$ for the (10, 10) nanotube, and $\delta n_{\rm sem} \simeq 1.7\%$ for the (11, 0) nanotube. Onset of the filling leads to sudden changes in the responses—obviously, a distortion $A_\perp$ that decreases the gap for the first band (say, with $q = 1$) would increase the gap for the second band (with $q = -2$). "Conflict of interests" of different bands is studied with the single band integral in Eq. (6) replaced with $\sum_i \int_0^{\delta k_i} \xi_i(k)\, dk$ over multiple bands i with appropriate boundaries δk_i. In Fig. 3 we show calculated $\gamma_\parallel$ for a series of carbon nanotubes as a function of the injection level. Sharp changes in the responses are clearly seen for the tubes (16, 0) and (17, 0). Within the same model, the dimensional response of graphite would be a smooth curve $\gamma_\parallel = \gamma_\perp = (\alpha/Kd)[2\sqrt{3}(\beta/\alpha)\delta n + \pi \delta n^2/3]$. The nanotube strains caused by charge injection fluctuate around the graphite curve, exhibiting the described sharp transitions. The amplitude of the fluctuations and the spacing between them decrease with the size of the nanotubes, gradually approaching the graphite response as $N, M \rightarrow \infty$.

In graphite, it is only the isotropic mode that gets excited upon charge injection leading to the isotropic expansion/contraction of the lattice. The quantization of electronic states in nanotubes makes anisotropic distortion modes a prominent feature of the accommodating

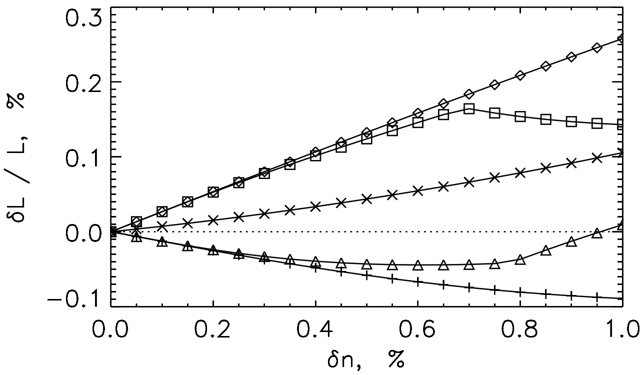

FIG. 3. Longitudinal dimensional changes for a series of electron doped nanotubes as a function of the injection level. Crosses are for the (10, 0) zigzag tube, diamonds for the (11, 0) tube, triangles for the (16, 0) tube, squares for the (17, 0) tube, and x's for the (10, 10) armchair tube. Lines here just connect the calculated data points.

lattice relaxation [15], especially so for semiconducting nanotubes. Equations (11) and data in Fig. 2 suggest that individual nanotubes can exhibit actuations larger by a factor of 3–4 than the graphite response. However, an oscillatory dependence on $N - M$ probably makes the observation of the larger effects difficult. For a bundle of nanotubes of various geometries, experiments [4] are likely to show some average, with larger strains from semiconducting tubes "compensating" each other. Separation of semiconducting nanotubes of the optimal type is therefore required to make the predicted enhancement practically useful. Proper selection of single nanotubes having large expansion coefficients would enable response optimization for nanoscale actuators.

Superimposed on the discussed effects can be a uniform expansion $\propto \delta n^2$ coming from the Coulomb repulsion of extra charges, whose magnitude depends on the positioning of counterions and dielectric properties of the medium. Coulombic intratube repulsion will likely dominate actuation when charge injected is large. The band structure effect will dominate either for low degrees of injected charge or where extra electrons and holes are introduced as a result of photoexcitation. Our results are relevant in such a system if extra charges quickly relax to the band edges and spend some time there. It should be reiterated that this Letter establishes only low temperature behavior in the single-electron picture. Evaluation of the effects of temperature [16] and *e*-*e* interactions [13] requires further studies.

In conclusion, we argued that SWNTs can display fascinating dimensional behavior as a result of lattice relaxation to accommodate extra electrons/holes at low injection levels. Large anisotropy in dimensional changes is predicted, possibly leading in some cases to decreasing diameter and increasing length upon charge injection. The oscillatory dependence of actuator strain on nanotube geometry is a dramatic predicted effect. For the same sign of carrier injection, some tubes may experience a longitudinal expansion, while others a contraction. Moreover, the electronic band structure of the nanotubes can reveal itself through sharp changes of the actuation response upon changing the doping level. Particularly strong dimensional changes are expected from semiconducting zigzag tubes, which may be substantially larger than the response of graphite.

This work was supported by DARPA Grant No. MDA972-02-C-005.

Note added.—*Ab initio* calculations on zigzag and armchair SWNTs (Ref. [17] and to be published) show that the strain as a function of charge per carbon approaches that of graphene for large radii. The deviations from the graphene behavior are found largest for semiconducting tubes with small radii, in agreement with the theory presented here. A detailed comparison of the results is underway and will be published elsewhere.

---

[1] R. Saito, G. Dresselhaus, and M. Dresselhaus, *Physical Properties of Carbon Nanotubes* (Imperial College Press, London, 1998).

[2] *Carbon Nanotubes: Synthesis, Structure, Properties and Applications,* edited by M. Dresselhaus, G. Dresselhaus, and P. Avouris (Springer, Berlin, 2000).

[3] R. Baughman, A. Zakhidov, and W. deHeer, Science (to be published).

[4] R. Baughman *et al.,* Science **284**, 1340 (1999).

[5] R. Schlittler, Science **292**, 1136 (2001).

[6] The energy of the undoped system is assumed to be included in the definition of its equilibrium lattice structure and vibrations; then it is a modulation of the energy of *additional* charges that is of interest to us.

[7] S. Hong and M. Kertesz, Phys. Rev. Lett. **64**, 3031 (1990).

[8] This implies a uniform distribution of excess charges over the lattice sites and relatively low temperatures. It is well known that one-dimensional electron-phonon systems can be unstable with respect to the Peierls distortion and exhibit formation of nonuniform polaronic distortions. For *not very small* carbon nanotubes, however, these effects seem practically irrelevant. The estimated transition temperatures (e.g., [9]) and polaron binding energies [9,10] are on the order of 1 K or smaller. So even quite low temperatures in excess of those estimates are sufficient to prevent nonuniform charge distributions. Of course, quantum fluctuations also act to render polaronic states unstable.

[9] C. Chamon, Phys. Rev. B **62**, 2806 (2000).

[10] M. Verissimo-Alves, R. B. Capaz, B. Koiller, E. Artacho, and H. Chacham, Phys. Rev. Lett. **86**, 3372 (2001).

[11] We use the units of length and energy such that the undistorted carbon-carbon bond length $d = 1/\sqrt{3}$ and the bare (isotropic) NNH integral $t_0 = 1$.

[12] C. Kane and E. Mele, Phys. Rev. Lett. **78**, 1932 (1997).

[13] L. Balents and M. Fisher, Phys. Rev. B **55**, R11 973 (1997).

[14] L. Yang and J. Han, Phys. Rev. Lett. **85**, 154 (2000).

[15] Inclusion of the longer range elastic interactions [1] is likely to enhance distortion anisotropy.

[16] We expect that thermal excitation of charges into higher lying energy bands will decrease the magnitude of enhanced dimensional changes (compare to the discussed effect of the increased injection level). Such an effect would be more significant for larger tubes. Since the separation between energy bands is large compared with thermal energy at room temperature for not too large nanotubes, we suspect that thermal corrections will be small at room temperature.

[17] M. Kertesz, G. Y. Sun, J. Kurti, and R. H. Baughman, Polym. Mater. Sci. Eng. **83**, 519 (2000).